ments were performed under continuous DC current with devices mounted on TO-5 headers. No heat sinking was employed. Fig. 2 shows the power as a function of current emitted from samples (a), (b) and (c). The detuned samples can be seen to give more power than the tuned sample over all currents. For the detuned devices, the peak external quantum efficiency is just over 6% for currents below 1mA, giving around 0.1mW, whilst at 5mA, the efficiency is still a modest 5.4%, giving 0.5mW of power. Even at 13mA, where the device emits 1mW of power, the efficiency is still 4%. The peak efficiency for the tuned device is 4.5% at currents below 1mA, giving around 0.1mW of power. To deliver 0.5mW of power, we find that a current of 8mA is required, and the efficiency is 3.2%. External wall-plug efficiencies are similar in value to those stated for external quantum efficiencies. Fig. 2 also shows the output power for the 4nm detuned sample under pulsed current injection, with a 10μs long current pulse and 1ms period. This indicates the increase in power that would be available if the device were to be adequately heat sunk.

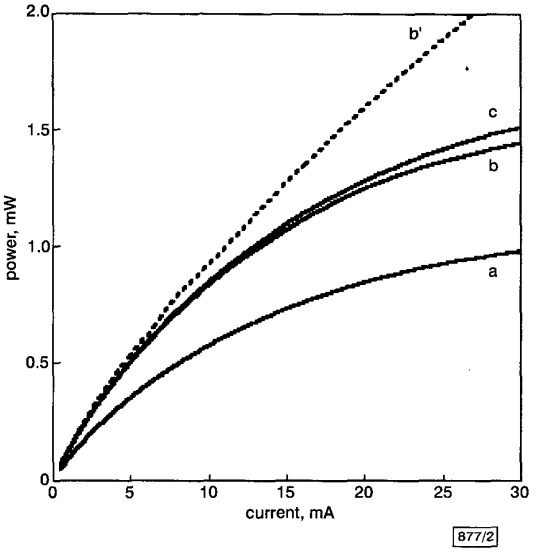

Fig. 2 *Output power for tuned, 4nm detuned and 6nm detuned RCLED under DC current injection*

a Tuned, DC current
b 4nm detuned, DC current
b' 4nm detuned sample under pulsed current injection, using 10μs long current pulse and 1ms period (giving 1% duty cycle)
c 6nm detuned, DC current

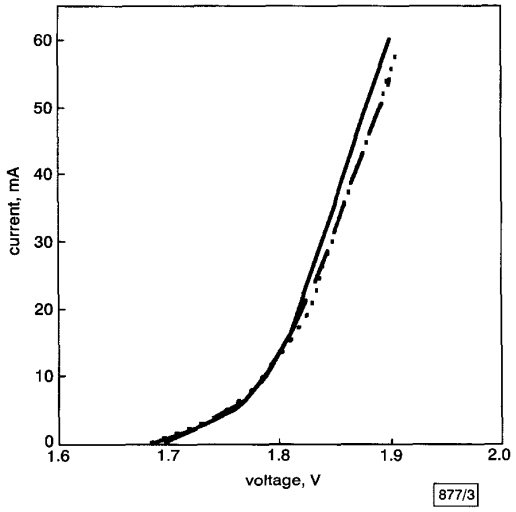

Fig. 3 *I/V characteristics for tuned, 4nm detuned and 6 nm detuned RCLED*

——— tuned
— · — 4nm detuned
····· 6nm detuned

Fig. 3 shows the I-V characteristics for the RCLEDs under forward bias. Voltages are between 1.7 and 1.9V in the current range 0–60mA. The low turn-on voltages are attributed to the high levels of carbon doping achieved in the *p*-type layers.

Conclusion: We have demonstrated high efficiency, low-voltage RCLEDs operating at 650 nm [Note 1].

Acknowledgments: The authors would like to thank G. Hill (Sheffield) for the processing of devices. This work is supported by the U.K. Engineering and Physical Sciences Research Council (EPSRC).

28 June 2000
Electronics Letters Online No: 20001182
DOI: 10.1049/el:20001182

J.W. Gray, Y.S. Jalili, P.N. Stavrinou, M. Whitehead and G. Parry (*Centre for Electronic Materials and Devices, The Blackett Laboratory, Imperial College of Science, Technology and Medicine, London SW7 2BZ, United Kingdom*)

A. Joel, R. Robjohn, R. Petrie, S. Hunjan, P. Gong and G. Duggan (*Epitaxial Products International Ltd., Cypress Drive, St. Mellons, Cardiff CF3 0EG, United Kingdom*)

References

1 DE NEVE, H., BLONDELLE, J., BAETS, R., DEMEESTER, P., VAN DAELE, P., and BORGHS, G.: 'High efficiency planar microcavity LED's: comparison of design and experiment', *IEEE Photonics Technol. Lett.*, 1995, **7**, (3), pp. 287–289

2 LOTT, J.A., SCHNEIDER, R.P., VAWTER, G.A., ZOLPER, J.C., and MALLOY, K.J.: 'Visible (660 nm) resonant-cavity light-emitting diodes', *Electron. Lett.*, 1993, **29**, (4), pp. 328–329

3 STREUBEL, K., HELIN, U., OSKARSSON, V., BäCKLIN, E., and JOHANSSON, Å.: 'High brightness visible (660 nm) resonant-cavity light-emitting diode', *IEEE Photonics Technol. Lett.*, 1998, **10**, (12), pp. 1685–1687

4 SNOWTON, P.M., and BLOOD, P.: '$GaInP$-$(Al_yGa_{1-y})InP$ 670 nm quantum-well lasers for high-temperature operation', *IEEE J. Quantum Electron.*, 1995, **31**, (12), pp. 2159–2164

5 STAVRINOU, P.N., WHITEHEAD, M., PARRY, G., and BUTTON, C.C.: 'Angular spectrum of visible resonant-cavity light-emitting diodes', *J. Appl. Phys.*, 1999, **86**, (6), pp. 3475–3477

6 SIPILÄ, P., SAARINEN, M., GUINA, M., VILOKKINEN, V., TOIVONEN, M., and PESSA, M.: 'Temperature behaviour of resonant cavity light-emitting diodes at 650 nm', *Semicond. Sci. Technol.*, 2000, **15**, pp. 418–421

Fast feedforward channel sounding RAKE receiver

Chun-Chyuan Chen and Chia-Chi Huang

A RAKE receiver with a feedforward channel sounding technique is described. Chip rate sampling is used to reduce the hardware complexity. A novel path-selection technique is employed to track the rapidly changing channel impulse response. The bit error rate performance of this RAKE receiver was evaluated by computer simulation.

Introduction: In a CDMA system, a RAKE receiver combats the effect of multipath fading by resolving and optimally combining major multipath components [1]. Within a conventional RAKE receiver, the pseudonoise (PN) code synchronisation is usually achieved in two steps, i.e. acquisition and tracking. Code acquisition achieves coarse code phase alignment, within a fraction of a chip period, between a locally generated PN code and a received PN code. Conversely, code tracking achieves fine code phase alignment between the two PN codes and it is usually implemented with a delay-locked loop (DLL) scheme [2]. Because a DLL scheme induces a delay from its feedback process, its

Note 1: Since the submission of this Letter, we have learned of a similar report describing 650nm RCLEDs grown by molecular beam epitaxy, which have comparable performance characteristics to the devices decribed here [6].

performance greatly degrades while a multipath channel changes rapidly.

In this Letter, we propose a fast feedforward channel sounding RAKE receiver. We adopt a novel path selection technique to track the fast changes of the multipath fading channel. The proposed receiver has low complexity and works well in a fast fading multipath channel.

System model: In a direct sequence spread spectrum (DS-SS) system, we assume a pilot signal is transmitted with a data signal to estimate the channel. The transmitted baseband signal $S^{(i)}(t)$ for the ith data symbol period can be represented by

$$S^{(i)}(t) = \sum_{n=0}^{N_p-1} \left(\sqrt{G_p}C_{p,n} + d^{(i)}C_{d,n}\right) \cdot P(t - nT_c) \quad (1)$$

where N_p is the length of the PN code, $\sqrt{G_p}$ is the gain of the pilot signal relative to the data signal, $C_{p,n}$ is the nth chip of the pilot PN code, $C_{d,n}$ is the nth chip of the data PN code, $d^{(i)}$ is the ith data symbol (+1 or −1), $P(t)$ is the transmitted pulse shaping function, and T_c is the chip period. We also assume the pulse shaping filters at the transmitter and the receiver are both squared root raised cosine filters. The transmitted signal is oversampled and sent through a multipath fading channel model which includes the effect of the two squared root raised cosine filters. We decimate the received signal into one sample per chip before it is fed to the proposed RAKE receiver.

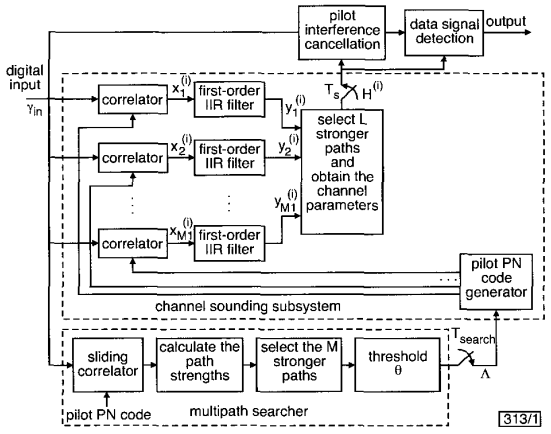

Fig. 1 *Proposed RAKE receiver*

Proposed RAKE receiver: As shown in Fig. 1, the proposed RAKE receiver includes a multipath searcher, a channel sounding subsystem, a pilot interference cancellation block, and a data signal detection block. The multipath searcher estimates the power delay profile of the multipath channel and sends it to the channel sounding subsystem every search period T_{search}. In the multipath searcher, we use a sliding correlator to despread the input signal γ_{in}. Since a sliding correlator generates a correlation result of the pilot PN code every N_pT_c period, it takes, in total, an $N_p^2\,T_c$ period to calculate the path strengths of N_p different code phase delays. To estimate a power delay profile reliably, we use a search period T_{search} which is a multiple of $N_p^2\,T_c$ period to obtain an averaged path strength at each individual codephase delay. After calculating the averaged path strengths, we select the M stronger paths out of the N_p estimated path strengths. To suppress further the weak paths, we discard those selected paths with strengths less than a threshold θ. The threshold θ is defined according to the peak value of the M selected paths, i.e. we obtain $M1$ ($M1 \le M$) output code phase delays ($\Lambda \equiv (k_1, k_2, ..., k_{M1})$) at the output of the multipath searcher.

In the channel sounding subsystem, the input signal γ_{in} is first fed to $M1$ correlators to despread the $M1$ selected paths in parallel. Afterwards, $M1$ first-order IIR filters are used to estimate each multipath component individually, i.e.

$$y_m^{(i)} = \alpha \cdot y_m^{(i-1)} + (1-\alpha) \cdot x_m^{(i)} \qquad m = 1, 2, ..., M1 \quad (2)$$

where $y_m^{(i)}$ is the estimated complex channel gain of the mth path at the ith symbol period, α defines the time constant of the IIR filter, and $x_m^{(i)}$ is the correlator output for the mth path at the ith symbol period. Out of the $M1$ estimated complex channel gains, we finally select the L stronger paths ($L \equiv \min(M1, L1)$, where $L1$ is a system parameter which defines the maximal number of the finally selected paths to be the estimated channel parameters for every symbol period T_s ($T_s = N_pT_c$). The finally estimated channel parameters ($H^{(i)} \equiv ([k'_1, y'^{(i)}_1], [k'_1, y'^{(i)}_1], ..., [k'_L, y'^{(i)}_L])$) contain both the estimated code phase delay k'_l and the estimated complex channel gain $y'^{(i)}_l$ for each finally selected multipath component.

To improve system performance, our RAKE receiver adopts pilot interference cancellation. According to the estimated channel parameters, the pilot signal can be reconstructed and subtracted from the received signal. In the data signal detection block, we despread the received data signal and use the maximal ratio combining technique to combine the L selected paths for data detection.

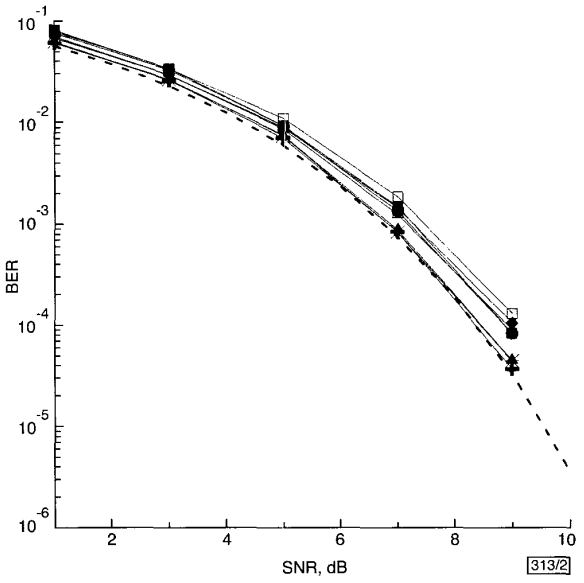

Fig. 2 *BER performance with α = 0.99 in fixed two-path channel*

- – – – theoretical BPSK performance
- —+— zero phase-shift
- —✳— phase-shift of 1/8 chip time
- —◆— phase-shift of 2/8 chip time
- —■— phase-shift of 3/8 chip time
- —□— phase-shift of 4/8 chip time
- —●— phase-shift of 5/8 chip time
- —△— phase-shift of 6/8 chip time
- —▲— phase-shift of 7/8 chip time

Simulation results: To evaluate the performance of the proposed RAKE receiver, computer simulations were carried out under different channel conditions. The binary phase-shift keying (BPSK) DS-SS modulation scheme at a data rate of 16kbit/s was assumed. The length of the PN code is 255. The roll-off factor of the squared root raised cosine filters at the transmitter and the receiver was set to 0.22. A two-path channel at a carrier frequency of 2GHz is assumed and the two paths assumed to have equal power. The delay between the two paths was set to an integer multiple of the chip time. We restricted the pilot power to 10% of the total transmission power, i.e. the pilot power gain G_p relative to the data power was set to ~7.5dB, assuming there are 50 channels with 100% activity and all channels are of equal power. In the multipath searcher, the number M of the selected paths was set to 8 and the threshold θ was set to 8dB below the peak power value of the M selected paths. The search period T_{search} was set to $10N_p^2\,T_c$. In the channel sounding subsystem, the maximal number $L1$ of the finally selected paths was set to 4.

To investigate the effect of the sampling phase-shifts on the performance of our RAKE receiver, we simulated at eight different sampling phase-shifts. Fig. 2 shows the bit error rate (BER) performance with $\alpha = 0.99$ in a fixed two-path channel. From Fig. 2, we observe that the RAKE receiver with a zero (ideal) sampling phase-shift achieves almost the same performance as the theoretical BPSK performance. For all the other sampling phase-shifts,

the performance degradation of the RAKE receiver is < 1dB in signal-to-noise ratio (SNR). Fig. 3 shows the BER performance with $\alpha = 0.5$ in a two-path Rayleigh fading channel at a vehicle speed of 120km/h. From Fig. 3, we observe that the RAKE receiver performs almost the same with different sampling phase-shifts. Contrasted with the theoretical BPSK performance [3], the performance degradation of the RAKE receiver is ~2dB in SNR at a BER of 10^{-3}.

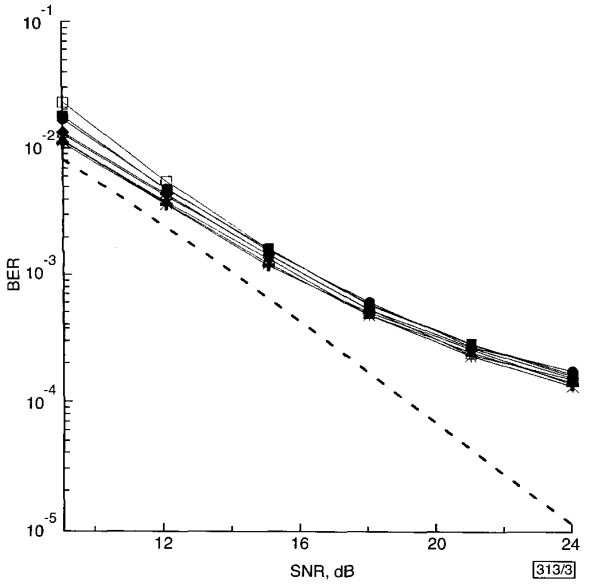

Fig. 3 *BER performance with $\alpha = 0.5$ in two-path Rayleigh fading channel at vehicle speed of 120km/h*

- – – – theoretical BPSK performance
- —+— zero phase-shift
- —✳— phase-shift of 1/8 chip time
- —◆— phase-shift of 2/8 chip time
- —■— phase-shift of 3/8 chip time
- —□— phase-shift of 4/8 chip time
- —●— phase-shift of 5/8 chip time
- —△— phase-shift of 6/8 chip time
- —▲— phase-shift of 7/8 chip time

Conclusions: In this Letter, a fast feedforward channel sounding RAKE receiver is presented. Instead of utilising a conventional tracking loop, we use a novel path selection technique to cope with the rapid changes of the channel impulse response. In addition, chip rate sampling can be used to reduce the hardware complexity of the RAKE receiver. Simulation results show that this RAKE receiver works well in a multipath fading channel even when a non-ideal sampling phase-shift occurs.

27 July 2000

Electronics Letters Online No: 20001187

DOI: 10.1049/el:20001187

Chun-Chyuan Chen and Chia-Chi Huang (*Wireless Communication Laboratory, Department of Communication Engineering, National Chiao-Tung University, 1001 Ta Hsueh Road, Hsinchu, Taiwan, Republic of China*)

E-mail: huangcc@nctu.edu.tw

References

1 TURIN, G.L.: 'Introduction to spread spectrum antimultipath techniques and their application to urban digital radio', *Proc. IEEE,* 1980, **68**, (3), pp. 328–353

2 BRAUN, W.R.: 'PN acquisition and tracking performance in DS/CDMA systems with symbol-length spreading sequences', *IEEE Trans. Commun.*, 1997, **45**, (12), pp. 1595–1601

3 GLISIC, S., and VUCETIC, B.: 'Spread spectrum CDMA systems for wireless communications' (Artech House, Boston, 1997), pp. 236–240

First-order and conditional statistics of rain attenuation fade slope

B.C. Gremont and D.L. Ndzi

In accordance with the assumptions of Maseng and Bakken, the distribution of rain fade slope on high frequency GSO links is calculated and its Cauchy approximation is presented. The conditional PDF of the fade slope is finally modelled for application to predictive rain fade mitigation techniques (FMTs).

Theoretical model and its approximation: This Letter attempts to justify theoretically recent results published in [1, 2]. The rate of change of rain attenuation, $s(t)$, encountered on satellite slant paths is commonly referred to as the fade slope, [1], and may be defined by

$$s(t) = [y(t + \Delta t) - y(t)]/\Delta t \quad (1)$$

The slope is a function of two rain attenuation samples, $y(t + \Delta t)$ and $y(t)$. Rain attenuation is commonly sampled at 1 Hz, thus if $\Delta t = 1$ [second] one may refer to the instantaneous fade slope. Since the marginal statistics of attenuation is widely accepted as lognormal, it is logical that the distribution of $y(t + \Delta t)$ and $y(t)$ is joint-lognormal i.e.

$$f(y(t+\Delta t), y(t)) = \frac{1}{2\pi\sigma^2 y(t+\Delta t)y(t)\sqrt{1-r^2}} \times \exp\left[-\frac{1}{2(1-r^2)}\left(\frac{(\ln y(t+\Delta t)-m)^2}{\sigma^2} - \frac{2r(\ln y(t+\Delta t)-m)(\ln y(t)-m)}{\sigma^2} + \frac{(\ln y(t)-m)^2}{\sigma^2}\right)\right] \quad (2)$$

According to the assumptions of the Maseng-Bakken model [3, 4], the two parameters (m, σ) define the statistics of rain attenuation on a satellite slant-path. It can be shown that the correlation factor in eqn. 2 is $r = [e^{\sigma^2 e^{-\beta|\tau|}-1}]/[e^{\sigma^2-1}]$, where β describes the dynamic properties of rain attenuation. In this Letter, all the results were obtained for $(m, \sigma) = (-1.4, 1.498)$ and $\beta = 1.65 \times 10^{-3}$. If we let $w(t) = y(t + \Delta t)$, then it can be shown that the joint PDF of $s(t)$ and $w(t)$ is (omitting the dependence on t):

$$f(s,y) = \frac{\Delta t}{2\pi\sigma^2(y-\Delta t\cdot s)y\sqrt{1-r^2}} \times \exp\left[-\frac{1}{2(1-r^2)}\left(\frac{(\ln(y-\Delta t\cdot s)-m)^2}{\sigma^2} - \frac{2r(\ln(y-\Delta t\cdot s)-m)(\ln y-m)}{\sigma^2} + \frac{(\ln y-m)^2}{\sigma^2}\right)\right] \quad (3)$$

The PDF of the fade slope, $s \in]-\infty, \infty[$, can be obtained by integrating eqn. 3 over all possible y, giving

$$f(s) = \int_{\max(\Delta t\cdot s,0)}^{\infty} \frac{\Delta t}{2\pi\sigma^2(y-\Delta t\cdot s)y\sqrt{1-r^2}} \times \exp\left[-\frac{1}{2(1-r^2)}\left(\frac{(\ln(y-\Delta t\cdot s)-m)^2}{\sigma^2} - \frac{2r(\ln(y-\Delta t\cdot s)-m)(\ln y-m)}{\sigma^2} + \frac{(\ln y-m)^2}{\sigma^2}\right)\right] dy \quad (4)$$

Fig. 1 shows the CDF (integral of eqn. 4) of the fade slope, which is compared to the output of a DSP rain synthesiser ([6]). The results show that there is a very good agreement. It is worth mentioning that a very good (and simpler) approximation to the integral of eqn. 4 is a Cauchy distribution given by

$$F(s) = \text{Prob}\{s \le s\} = \frac{1}{2} + \frac{1}{\pi}\cdot\arctan(K\cdot s) \quad (5)$$

where K is an empirical constant which will depend on the actual values of m, σ, β (i.e. on the particular location of the link). For our values, the best fit (obtained by a parametric search) is $K = 37.7$, in which case the CDF in eqn. 5 is virtually indistinguishable from those obtained either by simulation or from eqn. 4, see Fig. 1. The conditional PDF $f(s|y)$ is of practical interest to pre-